THE JOURNAL OF PHYSICAL CHEMISTRY LETTERS
A JOURNAL OF THE AMERICAN CHEMICAL SOCIETY

pubs.acs.org/JPCL

Letter

Distant Symmetry Control in Electron-Induced Bond Cleavage

T. P. Ragesh Kumar, P. Nag, M. Ranković, T. F. M. Luxford, J. Kočišek, Z. Mašín,* and J. Fedor*

Cite This: J. Phys. Chem. Lett. 2022, 13, 11136−11142

Read Online

ACCESS | Metrics & More | Article Recommendations | Supporting Information

ABSTRACT: We experimentally show that N−H bond cleavage in the pyrrole molecule following resonant electron attachment is allowed and controlled by the motion of the atoms which are not dissociating, namely, of the carbon-attached hydrogen atoms. We use this fact to steer the efficiency of this bond cleavage. In order to interpret the experimental findings, we have developed a method for locating all resonant and virtual states of an electron-molecule system in the complex plane, based on all-electron R-matrix scattering calculations. Mapping these as a function of molecular geometry allows us to separate two contributing dissociation mechanisms: a π^* resonance formation inducing strong bending deformations and a nonresonant σ^* mechanism originating in a virtual state. The coupling between the two mechanisms is enabled by the out-of-plane motion of the C−H bonds, and we show that it must happen on an ultrafast (few fs) time scale.

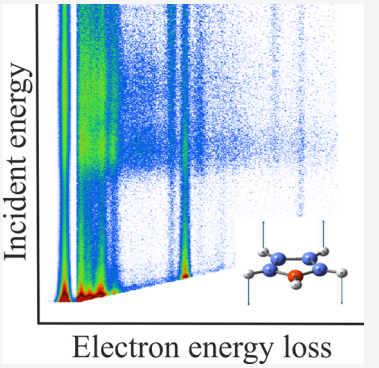

Downloaded via CHARLES UNIV IN PRAGUE on February 17, 2023 at 17:58:00 (UTC).
See https://pubs.acs.org/sharingguidelines for options on how to legitimately share published articles.

The most straightforward way that a molecular bond can be broken is by its direct prolongation without any other significant geometry change. In many cases, such a simple cleavage is symmetry forbidden. If the dissociation is initiated by a vertical transition, e.g., by an electron or photon impact, this type of situation arises when the initial state does not asymptotically correlate with the product states. In order for the bond to be broken, the molecular geometry must distort during the dissociation and thus lift the symmetry constraint.

This happens, for example, in dissociative electron attachment (DEA) to unsaturated organic molecules and biomolecules. Since DEA is a resonant process allowing for bond dissociation at subexcitation energies, it attracts significant interest in the fields of radiation damage to biological tissue[1] and drug metabolism.[2] It has been postulated for the C−H bond cleavage in acetylene[3] and HCN,[4] C−Cl bond cleavage in chlorobenzene,[5] and N−H bond cleavage in nucleobases[6] that the coupling between the entrance state (nondissociative π^*) and a dissociative state is mediated by an out-of-plane (or out-of-line) motion of the dissociating atom. It has been hypothesized that other molecular parts could be involved in the necessary symmetry lowering,[7,8] but such effect has never been experimentally proven. Here, we show that, in the pyrrole molecule, the motion of distant atoms influences the probability of bond cleavage. This effect can have significant consequences for the above-mentioned fields. Pyrrole is a heteroaromatic five-membered ring, which represents a common motif in biomolecules. It is highly symmetrical (C_{2v}) but complex, which allows us to control and decouple the symmetry-breaking and symmetry-preserving contributions to the dissociation.

Figure 1 shows a 2D electron energy loss (EELS) spectrum of pyrrole. The electrons collide with a molecule at an incident electron energy E_i (vertical axis) and leave with residual energy E_r. Their difference, the energy loss $\Delta E = E_i - E_r$, is plotted on the horizontal axis. The vertical trails thus correspond to the excitation of individual vibrations. Pyrrole has 24 normal modes.[9] Not all of them are fully resolved in the EELS experiment (resolution of 18 meV); however, several vibrations or their groups can be unambiguously assigned. The softest mode is the N−H out-of-plane bend (according to mode numbering from ref 9, ν_{16}, ΔE = 59 meV), and the stiffest is the N−H stretch (ν_1, ΔE = 437 meV). There is a prominent group of C−H out-of-plane bending vibrations (ν_{11}, ν_{13}, ν_{14}) centered around ΔE = 89 meV followed by other types of bending (ring deformations and C−H, N−H in plane bents). At 2.5 eV incident energy, the 2D spectrum clearly shows excitation of bending overtones.

Figure 1 also shows the excitation curves of selected vibrations. The IR active modes show threshold peaks which are common for polar molecules.[10] The threshold peak of the N−H stretch vibration ν_1 shows a sharp cusp at the energy which corresponds to the opening of the overtone excitation of this mode. This is evidence of a long-range electron−molecule interaction.[11,12] There are also three resonances, centered around 2.45, 3.5, and 7.5 eV (very broad). The first two are $\pi_1^*(b_1)$, $\pi_2^*(a_2)$. It will be shown below that the high-energy band is an overlap of $\sigma^*(a_1)$ and $\sigma^*(b_2)$. The two π^*

Received: October 11, 2022
Accepted: November 18, 2022
Published: November 28, 2022

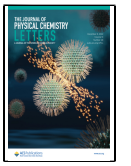

ACS Publications
© 2022 American Chemical Society

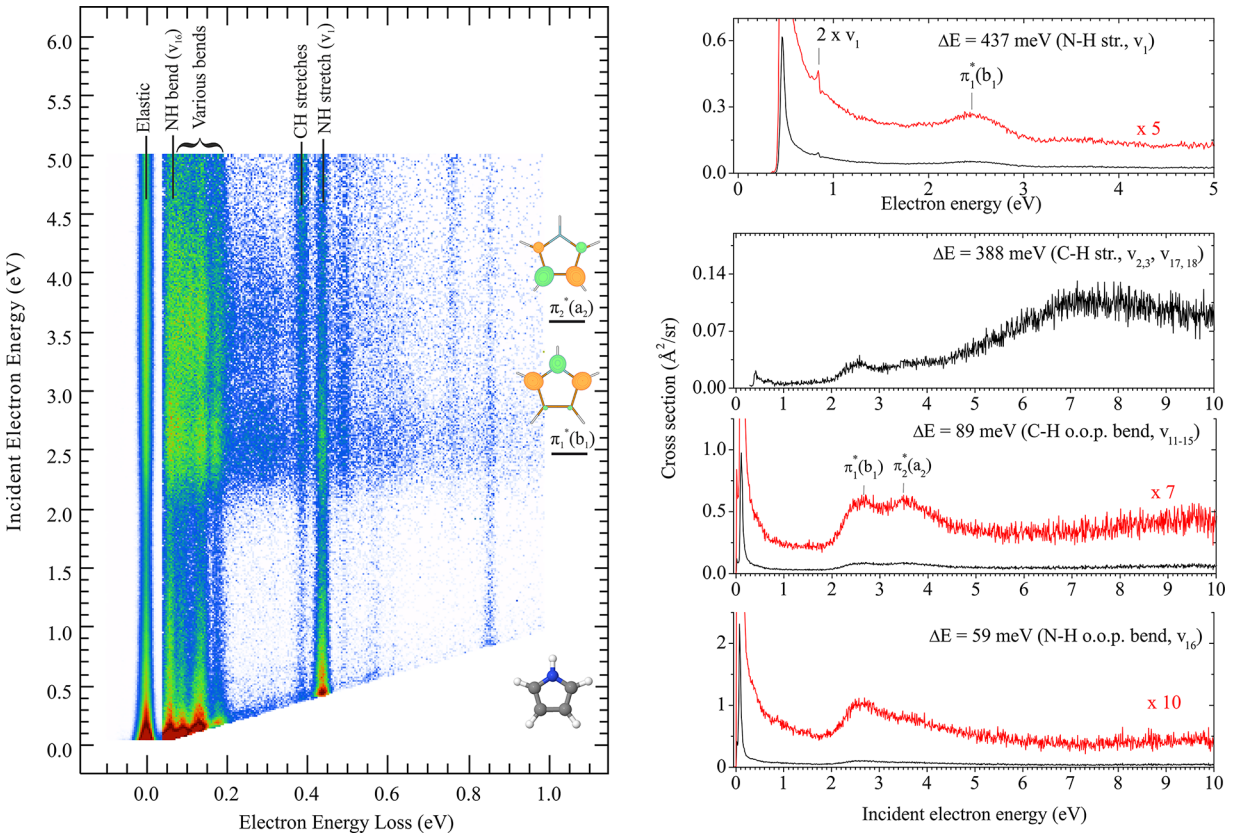

Figure 1. Two-dimensional electron energy loss spectrum of pyrrole (left) and the excitation curves of selected vibrations (intensity profiles) (right). The excitation curves were recorded separately in a longer energy range than the 2D spectrum. The N−H stretch vibration (top) is shown in a shorter energy range for better visibility of the marked cusp.

resonances were previously detected by electron transmission experiments[13,14] and calculations,[15,16] while the two σ^* resonances have been newly identified using our Siegert approach described below.

Figure 2 shows the DEA cross section for the N−H bond cleavage

$$C_4H_4NH + e^- \rightarrow C_4H_4N^- + H \quad (1)$$

The energy-integrated cross section (quantity independent of the instrumental resolution) is 2.19 pm^2 eV. The shape of the band agrees with previous reports of the relative ion yield.[17,18]

The DEA cross section is determined by the competition of the dissociation and electron detachment. If one prolongs the time scale for the dissociation, e.g., by replacing an H atom with deuterium, the dissociative cross section drops, since the electrons have more time to autodetach. In pyrrole, the cross section for the fully deuterated compound

$$C_4D_4ND + e^- \rightarrow C_4D_4N^- + D \quad (2)$$

is 0.09 pm^2 eV, almost a factor of 25 smaller than for reaction 1. Much more interestingly, the reaction

$$C_4D_4NH + e^- \rightarrow C_4D_4N^- + H \quad (3)$$

shows a cross section of 0.98 pm^2 eV, roughly 50% of reaction 1, even though it is still only the N−H bond which is dissociated. Such a strong drop cannot be caused by a slight difference in the reduced masses of the dissociating complex (see Supporting Information). Instead, the carbon-attached hydrogens have to play a crucial role in the cleavage of the N−H bond since their slowdown significantly reduces the DEA cross section. It should be noted that the dependence of the cross section on the dissociation time is extremely sensitive; in an early diatomic-like model of O'Malley[19] it is exponential (eq 1 in Supporting Information). The observed DEA cross section drop can thus be caused even by a small prolongation of the

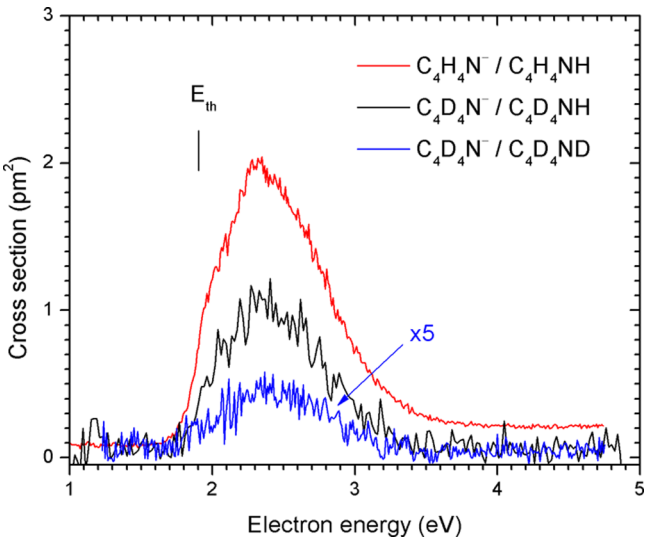

Figure 2. Dissociative electron attachment cross section for the N−H bond cleavage in pyrrole (red), fully deuterated pyrrole (blue), and pyrrole partially deuterated on the C-sites (black). The energetic threshold (E_{th}) for the process is marked.

https://doi.org/10.1021/acs.jpclett.2c03096
J. Phys. Chem. Lett. 2022, 13, 11136−11142

dissociation time. However, this prolongation has to be caused by slowing down the C−H (C−D) bonds.

The theory of dissociative electron attachment is complicated by the fact that the total energy of the system is in the scattering continuum, and the electronic wave function is not normalizable. Several types of states can play role in DEA. Shape resonances and virtual states are relevant in the present discussion, as they strongly affect electron scattering and DEA cross section. A shape resonance occurs when the electron−molecule interaction potential has a barrier which permits tunneling and the formation of a temporary bound state at a certain positive energy, while a virtual state appears close to the threshold and is typically associated with an emerging bound state.

Formally, these states can be thought of as a generalization of bound state solutions with outgoing-wave boundary conditions $\approx \exp[ik.r]$ but with k complex. This is the unified description of Siegert[21−24] where bound, resonant, and virtual states are treated on the same footing. In this formulation, bound states appear on the positive imaginary axis of momentum. Virtual and resonant states appear in the lower half complex plane of momentum and are therefore exponentially diverging solutions.

Some standard approaches from quantum chemistry upon their modification can be used to describe electronic resonances;[25−30] however, each has inherent limitations. Resonant and virtual states naturally appear in scattering methods which are able to describe wave functions extending over all space. This includes the R-matrix method,[20,31] Schwinger,[32] Kohn,[33] ePOLYSCAT,[34,35] and others.[36] Typically, those approaches are restricted to real scattering energies.

In this work, we have developed a method for locating and analyzing all Siegert states of the electron-molecule system in a unified way. The method is derived from the R-matrix approach for electron−molecule problems.[20,37] It uses a division of space to treat both exponentially decreasing (bound) and diverging (virtual, resonant state) distant parts of the Siegert state (N + 1 electron) wave function analytically, while the short-range part is described using configuration-interaction techniques including bound and continuum orbitals. Both wave function parts are matched on an R-matrix sphere large enough to fully contain the N-electron bound state of the target molecule.

The main results are shown in Figure 3. In the complex plane plot (here showing only the states in the $^2A_1$ symmetry), observable energy of a resonant state corresponds to its real part, its width is reflected in its imaginary part. There are several near-threshold and resonant states in the system. First, the two π^* resonances ($^2B_1$ at 2.32 eV and $^2A_2$ at 3.67 eV, shown in complex plane in Supporting InformationFigure 4). Second, there is a dipole-bound state (DBS) in $^2A_1$ symmetry. Third, there are two wide resonances of σ^* character ($^2A_1$ and $^2B_2$) which correlate with the wide peaks in the C−H stretch vibrational excitation above 6 eV (Figure 1). The valence bound state (VBS) of $^2A_1$ symmetry appears for larger N−H bond lengths. The calculations also show the presence of a large number of very wide Siegert states which are an inherent property of quantum scattering.[38]

DEA in pyrrole can proceed in the C_{2v} geometry without any symmetry breaking via a process which we will call *direct* σ^* *mechanism*, where only the N−H bond is stretched. It is the same process which has been postulated to occur in many polar biomolecules[15,39−45] and has been commonly denoted as

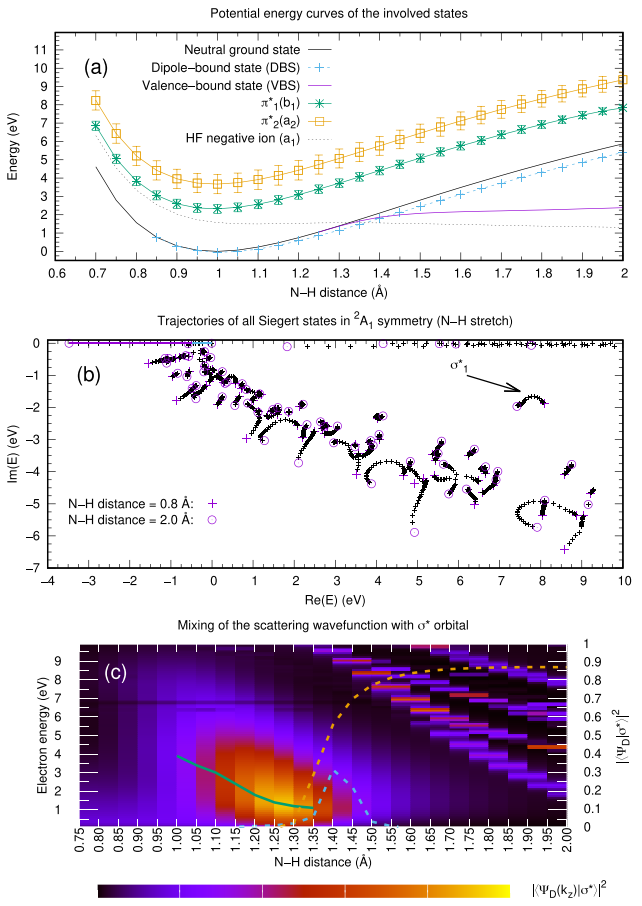

Figure 3. (a) Potential energy curves of the neutral, dipole-bound (DBS), valence-bound (VBS) states, and the two π^* resonances. Resonant energies and widths were obtained directly from the complex plane. The widths are indicated by the error bars. A curve for the lowest $^2A_1$ anion state at the Hartree−Fock (HF) level is shown for illustrative purposes. (b) All Siegert states of $^2A_1$ symmetry in the complex energy plane as a function of the N−H bond length. The points close to the real axis are unphysical pseudoresonances.[20] (c) Magnitude of the contribution of the σ^* orbital to the $^2A_1$ symmetry component of the scattering (Dyson-like) wave function for electron incoming in the direction of the N−H bond calculated as a function of the N−H bond distance and electron energy. The dashed orange and the dashed cyan line show the contribution of the σ^* orbital to the VBS and the DBS respectively.

being due to a very broad dipole-supported σ^* resonance. Its typical footprint is the sharp cusps in the vibrational excitation cross section such as observed in the N−H stretch excitation here. We find the usage of the term resonance in this process to be a source of confusion. In the present case it would be represented by a repulsive σ^*(N−H) state as exemplified in Figure 3a using the short dashed black line. However, no such state appears in Figure 3b: trajectories of all resonances (states with Re(E) > 0) are localized away from the real negative energy axis, and none of them are connected with the final VBS of the $^2A_1$ symmetry.

Instead, as Herzenberg showed for a model potential,[46] for dipole moments smaller than approximately 1.19 D, the VBS is connected with *unphysical* Riemann sheets of the momentum-space S-matrix. For larger and supercritical dipole moments, even this connection is lost, and the upper and lower half-planes remain decoupled.[46,47] We show in the Supporting

https://doi.org/10.1021/acs.jpclett.2c03096
J. Phys. Chem. Lett. 2022, 13, 11136−11142

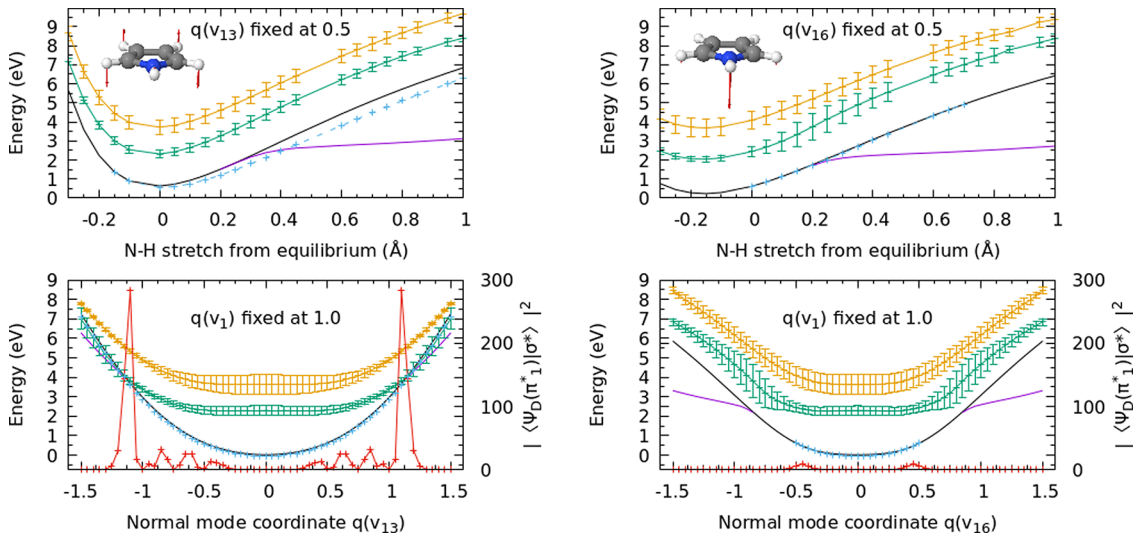

Figure 4. Involved states (same as in Figure 3) in the bent geometries. The modes ν_{13} (C−H bend), left, and ν_{16} (N−H bend), right, are depicted as insets. Top row: scans along the N−H stretch (ν_1) in the geometries distorted to $q = 0.5$ in the two bending modes. Bottom row: scans along the two bending modes with the N−H distance fixed to the equilibrium distance, $q(\nu_1) = 1$. The red curve shows the magnitude of mixing of the π_1^* resonant state with the lowest-lying σ^* orbital that describes the valence bound state for large N−H bond lengths.

Information in Section A.1 that when the long-range part of the electron-molecule interaction is removed (i.e., outside of the R-matrix sphere) and reduced to the short-range case these poles appear on the (single) momentum-space physical sheet of the S-matrix in the form of *subthreshold* virtual states. Therefore, while complicated in the complex momentum plane, physically, the formation of VBS in strongly polar molecules can be understood as the case of a virtual state becoming bound. Last but not least, this analysis demonstrates unambiguously that the higher-lying σ_1^* resonance is not needed to explain the σ^* DEA mechanism. When we evaluate the contribution of the σ^* orbital to the $^2A_1$ symmetry component of the scattering (Dyson-like) wave function for electron incoming in the direction of the N−H bond (Figure 3c, right axis), the trajectory of its maximal contribution (green line) resembles a repulsive potential curve dropping down to the threshold. Therefore, this state can be used conveniently to parametrize DEA in Feshbach-type methods,[48] but it does not correspond to any above-threshold resonant (Siegert) state.

Even though the direct σ^* DEA mechanism is open in pyrrole, it cannot explain the observed distant dissociation control which also involves other parts of the molecule. We thus examine the behavior of the π_1^* resonance upon breaking of the planar symmetry (Figure 4), especially as a function of the two most important ring-distorting vibrational modes ν_{13} (C−H out-of-plane) and ν_{16} (N−H out-of-plane). The flat character of the π_1^* resonance along these modes causes their efficient excitation. However, also in the broken symmetry this resonance remains nondissociative in the N−H stretch direction, as in the C_{2v} geometry. This is in contrast to the often assumed picture[15] described in the introduction, that bending opens the adiabatic dissociation pathway due to mixing of the π^* resonance with the repulsive state.

The involved states thus behave similarly as in the flat geometry. However, in the distorted geometries, the coupling between the resonance and the emerging valence bound state (described by the σ^* orbital, see Figure 3c) is allowed. Their mixing is represented by the red curve in Figure 4. The motion along the ν_{13} mode is much more efficient than ν_{16} at coupling to the σ^* mechanism (possibly because ν_{13} involves motion of four bonds, ν_{16} only of one). Additionally, the π_1^* width behaves differently in the two bending directions. For ν_{16}, the width increases in the region where the valence bound state forms. This leads to an enhanced detachment of electrons (this motion shakes the electrons off). The ν_{13} mode stabilizes the resonance (reduces its width and brings it closer in energy to the neutral state). It is reasonable to conclude that these factors combine to make ν_{13} motion more efficient at enhancing DEA cross section than the other modes. That makes the C−H motion the limiting step in the dynamics.

Finally, as we show in the Supporting Information, DEA in pyrrole is strongly directionally sensitive due to the different symmetries of the σ^* and π^* orbitals involved: the direct σ^* mechanism is maximized for electrons incoming along the NH bond, while the distant symmetry breaking mechanism proceeding via the π^* orbital requires electrons incoming from directions not in the molecular plane. This observation paves the way to disentangling both contributions and shows that the role of the π^* resonance is to temporarily capture electrons incoming from many different directions in order to give them enough time to "discover" the nonresonant σ^* pathway. This discovery time is limited by the resonance half-time, which in this case is approximately 5.5 fs. Therefore, the nuclear motion which is key for enabling DEA in pyrrole must occur on an ultrafast time scale of only a few femtoseconds.

We will now bring our results into context with previously observed phenomena related to π^*/σ^* coupling. Molecules with equilibrium geometries where the states are inherently mixed have much higher dissociative cross sections than molecules in which the states have to be dynamically coupled.[49] The efficiency of the bond-cleavage drops with the increasing distance (alkyl chains length) between the π^* system and the dissociating bond.[50] It also leads to puzzling temperature effects[51] and angular distributions.[52,53] The effect demonstrated here, coupling induced by motion of a distant molecular part, has been suggested,[7,8,54] but this is its first experimental evidence. However, all the prior works assumed

https://doi.org/10.1021/acs.jpclett.2c03096
J. Phys. Chem. Lett. 2022, 13, 11136−11142

that π^* states couple to repulsive shape resonances. We show that in pyrrole the coupling is with the emerging valence bound state.

A parallel can be drawn also with photochemistry. Upon photoexcitation of pyrrole into $\pi\sigma^*$ and $\pi\pi^*$ states, the vibronic coupling leads to quenching to the ground state and thus prevents dissociation.[15] Various forms of geometry distortions (including ring distortion) have been shown to play role in the photostabilization mechanism.[55,56] In principle, the current type of reaction control could be applied also to some photochemical (especially photoionization) reactions since autoionization continuum can couple to dissociative states.[57]

In conclusion, we have demonstrated that the N−H bond cleavage in pyrrole induced by low energy electrons is controlled by motion of the C−H bonds which are not being broken. Siegert-state analysis provides interpretation of this effect. The current findings:

- Resolve a long-standing discussion about the role of the σ^* mechanism in the DEA to polar biomolecules. While the postulation and parametrization of broad σ^* resonances has successfully reproduced DEA cross sections in many molecules,[39,41,42,58] the scattering calculations consistently fail to locate such resonances. The hypothesis has been that these are too far from the real axis (they are too broad) to be discerned. We show that in pyrrole, the σ^* mechanism is open, but it is nonresonant and is connected with the presence of a virtual state.
- Raise questions regarding DEA in biological systems (it is the only process in radiation damage which can cause bond breaking at energies lower than those of electronic excitation). The role of the environment has recently attracted a lot of attention with effects like mechanical caging,[59] changes of bond-cleavege patterns,[60] and even stereoselectivity[61] being identified. Due to the dissociation control identified here, the environment can also play role in inhibiting or amplifying the symmetry-breaking motion of peripheral parts of the molecule.
- Show the need for multidimensional and multistate models of resonant nuclear dynamics in polyatomic molecules which will be able to rationalize and predict this type of motion.

EXPERIMENTAL METHODS

The 2D electron-energy loss spectra (Figure 1) were measured on the electrostatic hemispherical spectrometer.[62,63] The electron energy scale was calibrated on the ^2S resonance in Helium at 19.366 eV, and the combined electron energy resolution was around 18 meV.

The absolute DEA cross sections for various pyrrole isotopomers (Figure 2) were measured using the quantitative DEA spectrometer with a time-of-flight analyzer.[64,65] The cross section in pyrrole was calibrated against the O^- cross section from CO_2 at 4.4 eV (13.3 pm^2 eV).[8] The error of the absolute value is estimated to be ±20%. The absolute cross sections of pyrrole isotopomers were then calibrated with respect to each other. Here we did short measurements of ion signal at four different energies across the DEA band and determined the signal ratios. The short acquisition times ensured high stability of electron current and sample pressures. The shape of the DEA band for each isotopomer was then measured on the DEA spectrometer with a quadrupole mass filter,[66] which has the electron energy resolution of approximately 70 meV. These spectra were normalized to the time-of-flight absolute values using the invariant of the energy-integrated cross sections.

The pyrrole and pyrrole-d_5 samples were purchased from Sigma-Aldrich, and pyrrole-d_4 was purchased from CDN-Isotopes. All samples had a stated purity of 98%. In both EELS and DEA experiments, the temperature of molecules in the collision region was 330 K.

THEORETICAL METHODS

We extend the R-matrix approach of Morgan and Burke[37,67] for the search of individual Siegert states to identification of all Siegert states in the complex plane and implement it into the UKRmol+ suite.[20] Briefly, the effective (generally complex) channel angular momenta λ_i were obtained by diagonalizing the matrix of the dipolar coupling coefficients including the diagonal channel angular momenta l_i. On this basis the outer region problem is decoupled, and its solution is analytic in the form of the incoming and outgoing wave complex spherical Hankel functions $H^{(\pm)}_{\lambda_i}(kr)$. The Siegert solution is the purely outgoing-wave solution which in the decoupled basis has the form:

$$H^{(+)}_{ij}(r) \underset{r\to\infty}{\sim} \delta_{i,j} e^{i(kr-\lambda_i\pi/2)} \tag{4}$$

S-matrix poles, including bound states, coincide with those complex momenta, k, for which Siegert solutions exist, i.e., momenta where the R-matrix matching condition is satisfied. See the Supporting Information for details of the numerical procedure.

ASSOCIATED CONTENT

Supporting Information

The Supporting Information is available free of charge at https://pubs.acs.org/doi/10.1021/acs.jpclett.2c03096.

Comparison of the resonance positions with the ones reported in the literature, estimate of the DEA cross section due to change in reduced mass, details of the theoretical model (PDF)

AUTHOR INFORMATION

Corresponding Authors

Z. Mašín − *Faculty of Mathematics and Physics, Charles University, Institute of Theoretical Physics, 18000 Prague, Czech Republic*; Email: zdenek.masin@utf.mff.cuni.cz

J. Fedor − *J. Heyrovský Institute of Physical Chemistry, The Czech Academy of Sciences, 18223 Prague, Czech Republic*; orcid.org/0000-0002-4549-9680; Email: juraj.fedor@jh-inst.cas.cz

Authors

T. P. Ragesh Kumar − *J. Heyrovský Institute of Physical Chemistry, The Czech Academy of Sciences, 18223 Prague, Czech Republic*

P. Nag − *J. Heyrovský Institute of Physical Chemistry, The Czech Academy of Sciences, 18223 Prague, Czech Republic*; orcid.org/0000-0002-1530-6104

M. Ranković − *J. Heyrovský Institute of Physical Chemistry, The Czech Academy of Sciences, 18223 Prague, Czech Republic*

https://doi.org/10.1021/acs.jpclett.2c03096
J. Phys. Chem. Lett. 2022, 13, 11136−11142

T. F. M. Luxford − *J. Heyrovský Institute of Physical Chemistry, The Czech Academy of Sciences, 18223 Prague, Czech Republic*

J. Kočišek − *J. Heyrovský Institute of Physical Chemistry, The Czech Academy of Sciences, 18223 Prague, Czech Republic;* orcid.org/0000-0002-6071-2144

Complete contact information is available at: https://pubs.acs.org/10.1021/acs.jpclett.2c03096

Notes

The authors declare no competing financial interest.

■ ACKNOWLEDGMENTS

This work is part of the Czech Science Foundation Projects 21-26601X (J.F.) and 20-15548Y (Z.M.) Z.M. also acknowledges support from Charles University (PRIMUS/20/SCI/003), OP RDE project CZ.02.2.69/0.0/0.0/16_027/0008495, the MEYS projects "e-Infrastructure CZ − LM2018140" and "IT4Innovations National Supercomputing Center - LM2015070". We thank R. Čurík, K. Houfek, and M. Čížek for stimulating discussions.

■ REFERENCES

(1) Gorfinkiel, J. D.; Ptasinska, S. Electron Scattering from Molecules and Molecular Aggregates of Biological Relevance. *Journal of Physics B: Atomic, Molecular and Optical Physics* **2017**, *50*, 182001.

(2) Pshenichnyuk, S. A.; Modelli, A.; Komolov, A. S.Interconnections Between Dissociative Electron Attachment and Electron-Driven Biological Processes. *Int. Rev. Phys. Chem.***2018**, *37*, 125−170,.

(3) Chourou, S. T.; Orel, A. E. Dissociative Attachment to Acetylene. *Phys. Rev. A* **2008**, *77*, 042709.

(4) Chourou, S. T.; Orel, A. E. Isotope effect in Dissociative Electron Attachment to HCN. *Phys. Rev. A* **2011**, *83*, 032709.

(5) Skalicky, T.; Chollet, C.; Pasquier, N.; Allan, M. Properties of the pi* and sigma* states of the chlorobenzene anion determined by electron impact spectroscopy. *Phys. Chem. Chem. Phys.* **2002**, *4*, 3583−3590.

(6) Burrow, P. D.; Gallup, G. A.; Scheer, A. M.; Denifl, S.; Ptasińska, S.; Märk, T.; Scheier, P. Vibrational Feshbach Resonances in Uracil and Thymine. *J. Chem. Phys.* **2006**, *124*, 124310.

(7) Rescigno, T. N.; Trevisan, C. S.; Orel, A. E. Dynamics of Low-Energy Electron Attachment to Formic Acid. *Phys. Rev. Lett.* **2006**, *96*, 213201.

(8) Janečková, R.; Kubala, D.; May, O.; Fedor, J.; Allan, M. Experimental Evidence on the Mechanism of Dissociative Electron Attachment in Formic Acid. *Phys. Rev. Lett.* **2013**, *111*, 203201.

(9) Mellouki, A.; Lievin, J.; Herman, M. The Vibrational Spectrum of Pyrrole and Furan in the Gas Phase. *Chem. Phys.* **2001**, *271*, 239−266.

(10) Itikawa, Y. Electron-Impact Vibrational Excitation of Polyatomic Molecules. *Int. Rev. Phys. Chem.* **1997**, *16*, 155−176.

(11) Hotop, H.; Ruf, M.-W.; Allan, M.; Fabrikant, I. In *Resonance and Threshold Phenomena in Low-Energy Electron Collisions with Molecules and Clusters*; Bederson, B., Walther, H., Eds.; Advances In Atomic, Molecular, and Optical Physics; Academic Press, 2003; Vol. *49*; pp 85−216.

(12) Fabrikant, I. I. Long-Range Effects in Electron Scattering by Polar Molecules. *J. Phys. B* **2016**, *49*, 222005.

(13) Modelli, A.; Burrow, P. D. Electron Attachment to the Aza-Derivatives of Furan, Pyrrole, and Thiophene. *J. Phys. Chem. A* **2004**, *108*, 5721−5726.

(14) Pshenichnyuk, S. A.; Fabrikant, I. I.; Modelli, A.; Ptasinska, S.; Komolov, A. S. Resonance Electron Interaction with Five-Membered Heterocyclic Compounds: Vibrational Feshbach Resonances and Hydrogen-Atom Stripping. *Phys. Rev. A* **2019**, *100*, 012708.

(15) de Oliveira, E. M.; Lima, M. A. P.; Bettega, M. H. F.; Sanchez, S. d'A.; da Costa, R. F.; Varella, M. T. d. N. Low-Energy Electron Collisions with Pyrrole. *J. Chem. Phys.* **2010**, *132*, 204301.

(16) Mukherjee, M.; Kumar, T. P. R.; Ranković, M.; Nag, P.; Fedor, J.; Krylov, A. I. Spectroscopic Signatures of States in the Continuum Characterized by a Joint Experimental and Theoretical Study of Pyrrole. *J. Chem. Phys.* **2022**, *157*, 204305 DOI: 10.1063/5.0123603.

(17) Skalický, T.; Allan, M. The Assignment of Dissociative Electron Attachment Bands in Compounds Containing Hydroxyl and Amino Groups. *J. Phys. B* **2004**, *37*, 4849.

(18) Muftakhov, M. V.; Asfandiarov, N.; Khvostenko, V. Resonant Dissociative Attachment of Electrons to Molecules of Five-Membered Heterocyclic Compounds and Lactams. *J. Electr. Spetroscopy Relat. Phenomena* **1994**, *69*, 165−175.

(19) O'Malley, T. F. Theory of Dissciative Attachment. *Phys. Rev.* **1966**, *150*, 14−29.

(20) Mašín, Z.; Benda, J.; Gorfinkiel, J. D.; Harvey, A. G.; Tennyson, J. UKRmol+: A Suite for Modelling Electronic Processes in Molecules Interacting with Electrons, Positrons and Photons Using the R-matrix Method. *Comput. Phys. Commun.* **2020**, *249*, 107092.

(21) Siegert, A. J. F. On the Derivation of the Dispersion Formula for Nuclear Reactions. *Phys. Rev.* **1939**, *56*, 750−752.

(22) Tolstikhin, O. I.; Ostrovsky, V. N.; Nakamura, H.Siegert Pseudostate Formulation of Scattering Theory: One-channel case. *Physical Review A*1998, *58*, 2077−2096.

(23) Batishchev, P. A.; Tolstikhin, O. I.Siegert Pseudostate Formulation of Scattering Theory: Nonzero Angular Momenta in the One-Channel Case. *Phys. Rev. A***2007**, *75*, 062704.

(24) Kukulin, V. I.; Krasnopolsky, V. M.; Horacek, J. In *Theory of Resonances: Principles and Applications*; Kukulin, V. I., Krasnopolsky, V. M., Horacek, J., Eds.; Reidel Texts in the Mathematical Sciences; Springer Netherlands: Dordrecht, 1989.

(25) Thodika, M.; Matsika, S. Projected Complex Absorbing Potential Multireference Configuration Interaction Approach for Shape and Feshbach Resonances. *J. Chem. Theory Comput.* **2022**, *18*, 3377.

(26) Herbert, J. M.*Reviews in Computational Chemistry Volume 28*; John Wiley & Sons, Ltd, 2015; pp 391−517, Section 8, https://onlinelibrary.wiley.com/doi/pdf/10.1002/9781118889886.ch8.

(27) Moiseyev, N. Quantum Theory of Resonances: Calculating Energies, Widths and Cross-Sections by Complex Scaling. *Phys. Rep.* **1998**, *302*, 212−293.

(28) Simons, J. Theoretical Study of Negative Molecular Ions. *Annu. Rev. Phys. Chem.* **2011**, *62*, 107−128.

(29) Jagau, T.-C.; Bravaya, K. B.; Krylov, A. I. Extending Quantum Chemistry of Bound States to Electronic Resonances. *Annu. Rev. Phys. Chem.* **2017**, *68*, 525−553.

(30) Santra, R.; Cederbaum, L. S. Non-Hermitian Electronic Theory and Applications to Clusters. *Phys. Rep.* **2002**, *368*, 1−117.

(31) Tennyson, J. Electron-Molecule Collision Calculations Using the R-matrix Method. *Phys. Rep.* **2010**, *491*, 29−76.

(32) da Costa, R. F.; Varella, M. T. d. N.; Bettega, M. H. F.; Lima, M. A. P. Recent Advances in the Application of the Schwinger Multichannel Method with Pseudopotentials to Electron-Molecule Collisions. *European Physical Journal D* **2015**, *69*, 1−24.

(33) Rescigno, T. N.; McCurdy, C. W.; Orel, A. E.; Lengsfield, B. H. In *Computational Methods for Electron—Molecule Collisions*; Huo, W. M., Gianturco, F. A., Eds.; Springer US: Boston, MA, 1995; pp 1−44.

(34) Gianturco, F. A.; Lucchese, R. R.; Sanna, N.Calculation of Low-Energy Elastic Cross Sections for Electron-CF4 Scattering. *J. Chem. Phys.***1994**, *100*, 6464−6471.

(35) Natalense, A. P. P.; Lucchese, R. R.Cross Section and Asymmetry Parameter Calculation for Sulfur 1s Photoionization of SF6. *J. Chem. Phys.***1999**, *111*, 5344−5348.

(36) Huo, W. M., Gianturco, F. A., Eds. *Computational Methods for Electron—Molecule Collisions*; Springer US; 1995.

(37) Morgan, L. A.; Burke, P. G. Low-Energy Electron Scattering by HF. *Journal of Physics B: Atomic, Molecular and Optical Physics* **1988**, *21*, 2091−2105.

(38) Nussenzveig, H. The Poles of the S-matrix of a Rectangular Potential Well of Barrier. *Nucl. Phys.* **1959**, *11*, 499−521.
(39) Gallup, G. A.; Burrow, P. D.; Fabrikant, I. I. Electron-Induced Bond Breaking at Low Energies in HCOOH and Glycine: The Role of Very Short-Lived σ^* Anion States. *Phys. Rev. A* **2009**, *79*, 042701.
(40) Gallup, G. A.Role of a Short-Lived σ^* Resonance in Formic-Acid O—H Bond Breaking. *Phys. Rev. A***2013**, *88*, 052705,
(41) Gallup, G. A.; Fabrikant, I. I. Vibrational Feshbach Resonances in Dissociative Electron Attachment to Uracil. *Phys. Rev. A* **2011**, *83*, 012706.
(42) Fabrikant, I. I. Theory of Dissociative Electron Attachment: Biomolecules and clusters. *EPJ. Web of Conferences* **2015**, *84*, 07001.
(43) Scheer, A. M.; Aflatooni, K.; Gallup, G. A.; Burrow, P. D. Bond Breaking and Temporary Anion States in Uracil and Halouracils: Implications for the DNA Bases. *Phys. Rev. Lett.* **2004**, *92*, 068102.
(44) McAllister, M.; Kazemigazestane, N.; Henry, L. T.; Gu, B.; Fabrikant, I.; Tribello, G. A.; Kohanoff, J. Solvation Effects on Dissociative Electron Attachment to Thymine. *J. Phys. Chem. B* **2019**, *123*, 1537−1544.
(45) Scheer, A.; Silvernail, C.; Belot, J.; Aflatooni, K.; Gallup, G.; Burrow, P. Dissociative Electron Attachment to Uracil Deuterated at the N1 and N3 Positions. *Chem. Phys. Lett.* **2005**, *411*, 46−50.
(46) Herzenberg, A.; Saha, B. C. The virtual Electron State in a Weakly Polar Molecule. *Journal of Physics B: Atomic and Molecular Physics* **1983**, *16*, 591−602.
(47) Estrada, H.; Domcke, W.Analytic Properties of the S Matrix for a Simple Model of Fixed-Nuclei Electron-Polar-Molecule Scattering. *Journal of Physics B: Atomic and Molecular Physics***1984**, *17*, 279−297.
(48) Domcke, W. Theory of Resonance and Threshold Effects in Electron-Molecule Collisions: The Projection-Operator approach. *Phys. Rep.* **1991**, *208*, 97−188.
(49) Stricklett, K.; Chu, S.; Burrow, P. Dissociative Attachment in Vinyl and Allyl Chloride, Chlorobenzene and Benzyl Chloride. *Chem. Phys. Lett.* **1986**, *131*, 279−284.
(50) Aflatooni, K.; Gallup, G. A.; Burrow, P. D. Dissociative Electron Attachment in Nonplanar Chlorocarbons with pi*/sigma*-Coupled Molecular Orbitals. *J. Chem. Phys.* **2010**, *132*, 094306.
(51) Mahmoodi-Darian, M.; Denifl, S.; Probst, M.; Huber, S. E.; Mauracher, A.; Scheier, P.; Märk, T. D. Dissociative Electron Attachment to 2-Chlorotoluene: Unusual Temperature Effects for the Formation of Cl-. *Chem. Phys. Lett.* **2019**, *730*, 527−530.
(52) Fogle, M.; Haxton, D. J.; Landers, A. L.; Orel, A. E.; Rescigno, T. N. Ion-Momentum Imaging of Dissociative-Electron-Attachment Dynamics in Acetylene. *Phys. Rev. A* **2014**, *90*, 042712.
(53) Nag, P.; Tarana, M.; Fedor, J. Effects of pi*-sigma* Coupling on Dissociative-Electron-Attachment Angular Distributions in Vinyl, Allyl, and Benzyl Chloride and in Chlorobenzene. *Phys. Rev. A* **2021**, *103*, 032830.
(54) Kossoski, F.; Barbatti, M. Nonadiabatic Dynamics in Multi-dimensional Complex Potential Energy Surfaces. *Chem. Sci.* **2020**, *11*, 9827.
(55) Vallet, V.; Lan, Z.; Mahapatra, S.; Sobolewski, A. L.; Domcke, W. Photochemistry of Pyrrole: Time-Dependent Quantum Wave-Packet Description of the Dynamics at the pi simga*-S0 Conical Intersections. *J. Chem. Phys.* **2005**, *123*, 144307.
(56) Karsili, T. N. V.; Marchetti, B.; Moca, R.; Ashfold, M. N. R. UV Photodissociation of Pyrroles: Symmetry and Substituent Effects. *J. Phys. Chem. A* **2013**, *117*, 12067−12074.
(57) Larsen, K. A.; Lucchese, R. R.; Slaughter, D. S.; Weber, T. Distinguishing Resonance Symmetries with Energy-Resolved Photo-ion Angular Distributions from Ion-Pair Formation in O_2 Following Two-Photon Absorption of a 9.3 eV Femtosecond Pulse. *J. Chem. Phys.* **2020**, *153*, 021103.
(58) Vizcaino, V.; Puschnigg, B.; Huber, S. E.; Probst, M.; Fabrikant, I. I.; Gallup, G. A.; Illenberger, E.; Scheier, P.; Denifl, S. Hydrogen Loss in Aminobutanoic Acid Isomers by the sigma* Resonance Formed in Electron Capture. *New J. Phys.* **2012**, *14*, 043017.
(59) Kočišek, J.; Pysanenko, A.; Fárník, M.; Fedor, J. Microhydration Prevents Fragmentation of Uracil and Thymine by Low-Energy Electrons. *J. Phys. Chem. Lett.* **2016**, *7*, 3401−3405.
(60) Kočišek, J.; Sedmidubská, B.; Indrajith, S.; Fárník, M.; Fedor, J. Electron Attachment to Microhydrated Deoxycytidine Monophosphate. *J. Phys. Chem. B* **2018**, *122*, 5212−5217.
(61) Nogly, P.; Weinert, T.; James, D.; et al. Retinal Isomerization in Bacteriorhodopsin Captured by a Femtosecond X-ray Laser. *Science* **2018**, *361*, 6398.
(62) Allan, M. Measurement of Absolute Differential Cross Sections for Vibrational Excitation of O_2 by Electron Impact. *J. Phys. B: At. Mol. Opt. Phys.* **1995**, *28*, 5163.
(63) Allan, M. Measurement of the Elastic and $v = 0 \rightarrow 1$ Differential Electron-N_2 Cross Sections over a Wide Angular Range. *J. Phys. B: At. Mol. Opt. Phys.* **2005**, *38*, 3655−3672.
(64) May, O.; Fedor, J.; Allan, M. Isotope Effect in Dissociative Electron Attachment to Acetylene. *Phys. Rev. A* **2009**, *80*, 012706.
(65) Nag, P.; Polášek, M.; Fedor, J. Dissociative Electron Attachment in NCCN: Absolute Cross Sections and Velocity-Map Imaging. *Phys. Rev. A* **2019**, *99*, 052705.
(66) Stepanović, M.; Pariat, Y.; Allan, M. Dissociative Electron Attachment in Cyclopentanone, γ-Butyrolactone, Ethylene Carbonate and Ethylene Carbonate-d_4: Role of Dipole-Bound Resonances. *J. Chem. Phys.* **1999**, *110*, 11376.
(67) Morgan, L. A. Virtual States and Resonances in Electron Scattering by CO_{2}. *Phys. Rev. Lett.* **1998**, *80*, 1873−1875.

Recommended by ACS

Few-Femtosecond $C_2H_4^+$ Internal Relaxation Dynamics Accessed by Selective Excitation
Matteo Lucchini, Mauro Nisoli, *et al.*
NOVEMBER 29, 2022
THE JOURNAL OF PHYSICAL CHEMISTRY LETTERS
READ

Probing Isomerization Dynamics via a Dipole-Bound State
Yuzhu Lu, Chuangang Ning, *et al.*
SEPTEMBER 12, 2022
THE JOURNAL OF PHYSICAL CHEMISTRY LETTERS
READ

Spectroscopy and Theoretical Modeling of Tetracene Anion Resonances
Cole R. Sagan, Etienne Garand, *et al.*
OCTOBER 27, 2022
THE JOURNAL OF PHYSICAL CHEMISTRY LETTERS
READ

Ultrafast Charge and Proton Transfer in Doubly Ionized Ammonia Dimers
Jiaqi Zhou, Petr Slavíček, *et al.*
NOVEMBER 09, 2022
THE JOURNAL OF PHYSICAL CHEMISTRY LETTERS
READ

Get More Suggestions >

https://doi.org/10.1021/acs.jpclett.2c03096
J. Phys. Chem. Lett. 2022, 13, 11136−11142